Implementing visible 473 nm photodissociation in a Q-Exactive mass spectrometer: towards specific detection of cysteine-containing peptides

Marion Girod, Jordane Biarc, Quentin Enjalbert, Arnaud Salvador, Rodolphe Antoine, Philippe Dugourd, Jérôme Lemoine

Implementing visible 473 nm photodissociation in a Q-Exactive mass spectrometer: towards specific detection of cysteine-containing peptides

Marion Girod [a, b*+], *Jordane Biarc* [a, b*], *Quentin Enjalbert* [a,b,c], *Arnaud Salvador* [a, b], *Rodolphe Antoine* [a, c], *Philippe Dugourd* [a,c], *Jérôme Lemoine* [a,b]

[a] Université de Lyon, F-69622, Lyon, France ;

[b] CNRS et Université Lyon 1 UMR 5280, ISA

[c] CNRS et Université Lyon 1, UMR5306, ILM

[*] These authors contributed equally to this work

[+]**To whom correspondence should be addressed:**

Marion Girod: marion.girod@univ-lyon1.fr

Running title: photodissociation in a Q-Exactive.

ABSTRACT

Improvement of the fragmentation specificity may streamline data processing of bottom-up proteomic experiments by drastically reducing either the amount of MS/MS data to process in the discovery phase or the detection of interfering signals in targeted quantification. Photodissociation at proper wavelengths is a promising alternative technique to the non-discriminating conventional activation mode by collision. Here, we describe the implementation of visible LID at 473 nm in a Q-Exactive-Orbitrap mass spectrometer for the specific detection of cysteine-containing peptides tagged with a Dabcyl group. HCD cell DC offset and irradiation time were optimized to obtain high fragmentation yield and spectra free of contaminating CID product ions, while keeping the irradiation time scale compatible with chromatographic separation. With this optimized experimental set-up, the selective detection of cysteine-containing peptides in a whole tryptic hydrolysate of three combined proteins is demonstrated by comparing all ion fragmentation (AIF) spectra recorded online with and without laser irradiation.

Keywords

Photodissociation, high resolution mass spectrometer, cysteine-containing peptides, chromophore derivatization.

Introduction

Liquid chromatography coupled to peptide fragmentation by tandem mass spectrometry (MS/MS) is the pivotal analytical set-up for protein identification and quantification in proteomic workflows.[1] Most of these workflows use a non-selective activation mode applied to either successively filtered small windows of *m/z* value (data dependent acquisition), which ideally select unique precursor ions[2] or to larger *m/z* windows (data independent acquisition) where multiple precursor ions are simultaneously fragmented. While in the first case minor diluted compounds are often not sampled due to too slow acquisition frequency, the second mode is deals with a complex interpretation of composite MS/MS data.

Collision-induced dissociation (CID) remains the widespread technique to dissociate peptides of relatively small size after trypsin digestion. On the other hand, electron capture dissociation (ECD) and electron transfer dissociation (ETD)[3] have shown considerable interest for large peptide sequencing[4] and post-translational modification positioning on the peptide backbone.[5] Since all these activation methods are non-discriminative, conventional proteomic workflows lead to the data processing of huge amounts of fragment ion spectra, often redundant and most of the time resulting from the concomitant dissociation of multiple precursor ions due to co-eluted peptides. In a targeted quantification configuration, the high complexity and dynamic range of the peptide concentration in whole tryptic hydrolysate make the detection of minor proteins by these non-discriminating fragmentation techniques also very challenging. Protein fractionation either based on their physical properties or cellular localization can be done to improve dynamic range. Moreover, different strategies have been proposed to target a subset of a proteome by, for instance, focusing only on glycopeptides[6, 7] or cysteine-containing peptides after selective enrichment.[8]

Many reports have illustrated the promising potential of laser photodissociation to introduce

more specificity during the fragmentation step.[9-11] Compared to collisional activation, laser-induced dissociation (LID) enables specific excitation. Selecting the appropriate wavelength, naturally-absorbing native species or molecules tagged with proper chromophores may indeed be specifically excited. For instance, infrared multiphoton photodissociation at 10.6 μm has shown interesting propensity to differentiate phospho- and non-phosphorylated peptides[12] due to increased photon absorption of the phosphate group. LID in the UV range also delivers excellent versatility because the absorption of native biomolecules depends on their electronic properties, in particular on their natural chromophores.[13] As an illustration, Joly at al. documented specific cleavage of the C_α–C_β bond of tyrosyl residue under UV photodissociation of tyrosyl-containing peptides at 262 nm.[14] Julian et al. have documented the excitation of S-S and C-S bonds by 266 nm photons that may be exploited for the detection of disulfide bond partners.[15] This group similarly described the use of excitation at 266 nm for the detection and location of reduced cysteine in peptides or proteins after derivatization with a quinone group,[16] or the identification of the phosphorylation site combining β-elimination followed by Michael addition of a naphtalenethiol chromophore.[17] Note however that fragmentation specificity is not the only issue when considering photodissociation as an alternative method to CID. In fact, the irradiation time should also provide a sufficient fragmentation yield in order to make the sampling time and chromatographic peak definition compatible. This compatibility was recently shown by Brodbelt et al. by describing LC-MS platform coupled to on-line photodissociation for the analysis of whole proteins[18, 19] or tryptic hydrolysates[20] using high resolution detection. Recently, derivatization of specific amino acid residues in conjunction with selective photodissociation of the derivatized targeted peptides provides a streamlined approach to shotgun proteomics. Using excitation at 351 nm, only the cysteine-containing peptides grafted with Alexa Fluor 350 undergo extensive backbone fragmentation thus facilitating their

detection among their non-derivatized congeners.[21] The same experimental set-up also proved to be efficient in streamlining the detection of peptides tagged with a sulfo-NHS amine reactive chromophore group, which probes the accessibility of lysine residues at the protein surface.[22] Specific photodissociation was also obtained for Tyr/His-containing peptides after derivatization with diazonium chromophore groups.[23]

Detection specificity is also critical when tackling protein quantification in whole proteome by targeted mass spectrometry in selected reaction monitoring mode (SRM). We recently introduced a new technique called photo-SRM where visible LID at 473 nm was implemented in a hybrid quadrupole linear ion trap instrument.[24] Specific photodissociation is obtained for cysteine-containing peptides tagged with a Dabcyl group. Moreover, cysteine derivatization by hydrophobic and basic tags such as the Dabcyl chromophore induces an improved ionization yield and a reduced matrix effect.[25] Thus, photo-SRM showed similar or even improved detection performance compared to conventional CID-SRM for the analysis of a whole plasma hydrolysate.

In the present work, we describe the setup and optimization of LID at 473 nm coupled to a hybrid quadrupole-orbitrap Q-exactive instrument with the aim of developing a new proteomic strategy based on specific detection of the subset of cysteine-containing peptides in whole tryptic hydrolysate. Targeting only cysteine-containing peptides might indeed simplify peptide assignments in DIA mode since cysteine is a rare amino acid encountered at a frequency of about 2% in the human proteome.[26] Indeed, only 17.2% of tryptic peptides contain one or more cysteine residues. However, since 96% of the putative human proteins contain at least one cysteine residue and 60% bear at least two,[26] a significant part of the human proteome might, in theory, be covered. Therefore, both a HCD (High Collision Dissociation) cell DC offset (CE value) and activation time were optimized to ultimately

achieve the highest LID yield in a time scale amenable to chromatographic separation, while keeping the "all ion fragmentation" (AIF) spectra free of CID "contaminations". Besides classical backbone fragmentations, LID of cysteine-containing peptides tagged with a Dabcyl chromophore systematically induces the formation of a reporter ion at *m/z* 252, which helps streamlining the cysteine-containing peptide subset.

Materials and methods

Chemicals and reagents

Acetonitrile (ACN), methanol (MeOH) and water (LC–MS grade) were obtained from Fisher Scientific (Strasbourg, France). Dithiothreitol (DTT), iodoacetamide (IAM), formic acid (FA) (LC–MS grade), Trypsin (type IX-S from Porcine Pancreas), ammonium bicarbonate (AMBIC), tris(2-carboxyethyl)phosphine (TCEP), ammonium acetate (AA) were purchased from Sigma–Aldrich (St Quentin-Fallavier, France). The chromophore DABCYL C2 maleimide was purchased from AnaSpec (Fremont, CA). Prostate Specific Antigen (PSA) proteotypic peptide (IVGGWECEK) was synthesized by Millegen (Labège, France). Human Albumin, human serotransferin, chicken lysozyme were purchased from Sigma–Aldrich (St Quentin-Fallavier, France).

Instrumentation

Experiments were performed on an hybrid quadrupole-orbitrap Q-Exactive® mass spectrometer (Thermo Fisher Scientific, San Jose, CA, USA) equipped with a HESI ion source coupled to a Surveyor HPLC-MS pump (Thermo Fisher Scientific, San Jose, CA, USA) and a PAL Auto-sampler (CTC Analytics, Switzerland). This instrument has been modified to allow visible laser irradiation of ion molecules. A schematic of the photodissociation set-up is given in Figure 1. A quartz window was fitted on the rear of the

HCD (High Collision Dissociation) cell to permit introduction of a laser beam. The detector plate, initially positioned at the exit of the HCD cell and on the laser beam trajectory, was removed with no impact on the instrument performance (resolution and sensitivity). The laser is a 473 nm continuous wavelength laser (cw) (ACAL BFI, Evry, France). Its output power is tunable from 0 to 500 mW and its beam diameter is 1.5 mm (divergence 1 mrad). The laser beam passes through one diaphragm and is injected in the HCD cell using two mirrors. The laser is slightly off-axis in order to avoid photofragmentation in the C-trap. For photodissociation analyses, the continuous laser is permanently turned on.

Sample Preparations

In order to optimize the HCD cell parameters for the photodissociation, derivatized PSA proteotypic peptide (IVGGWECEK) was used as the standard molecule. IVGGWECEK peptide, at a concentration of 10 µg/mL, was reduced and derivatized with a 3-fold molar excess solution of TCEP (0.1 mg/mL in a 60 mM AA solution) and a 5-fold molar excess of DABCYL C2 maleimide chromophore (structure shown in Figure 2) in MeOH (1.33 µg/mL in MeOH). The mixture was stirred in the sonic bath then stored in the dark for 4h at room temperature.

For the specific detection of cysteine-containing peptides by photodissociation, albumin, serotransferin and lysozyme were derivatized with DABCYL C2 maleimide. The 3 proteins (7.5 nmol each) were dissolved in 3 000 µL of a 3-fold molar excess solution of TCEP (0.1 mg/mL in a 60 mM AA solution). Then, 3 000 µL of a 5-fold molar excess of DABCYL C2 maleimide in MeOH (0.5 mg/mL in MeOH) was added. The mixture was stirred in the sonic bath then stored in the dark for 4h at room temperature. The samples were diluted with 3ml of a 60 mM AA solution prior to overnight digestion at 37°C with trypsin using a 1:30 (w/w) enzyme to substrate ratio. Digestion was stopped by addition of formic acid to a final

concentration of 0.5%. All samples were desalted and concentrated using Oasis^{TM} HLB 3cc (60mg) reversed-phase cartridges (Waters, Milford, MA, USA). Before loading the tryptic digest onto the Oasis cartridges, all cartridges were conditioned with 1 mL of MeOH and then 1 mL of water containing 0.5% FA. After the loading, all cartridges were washed with 1 mL of MeOH/water (5/95, v/v) containing 0.5% FA and eluted with 2 mL of ACN containing 0.5% FA. All samples were evaporated to dryness and resuspended in 100 µL of water/MeOH (2:1, v/v) containing 0.5% FA. The final concentration of proteins was 750 µg/mL. All solutions were stored at -18°C prior to use.

HPLC separation

HPLC separation was carried out on an XBridge C_{18} column (100 X 2.1 mm, 3.5 µm) from Waters. The HPLC mobile phase consisted of water containing formic acid 0.1 % (v/v) as eluent A, and ACN containing formic acid 0.1% (v/v) as eluent B. Elution was performed at a flow rate of 300 µL/min. The PSA proteotypic peptide was eluted with 40 % of eluent B over 7 min. The elution sequence, for the 3 protein mixture, included a plateau with 20 % of eluent B for 5 min followed by a linear gradient from 20 % to 45 % for 33 min, then a plateau at 95 % of eluent B for 5 min. The gradient was returned to the initial conditions and held there for 7 min. The injection volume was 10 µL.

Mass Spectrometry Operating Conditions

Ionization was achieved using electrospray in positive ionization mode with an ion spray voltage of 4 500 V. The sheath gas and auxiliary gas (nitrogen) flow rates were set at 48 and 20 (arbitrary unit), respectively, with a HESI vaporizer temperature of 410°C. The ion transfer capillary temperature was 250°C with a sweep gas (nitrogen) flow rate at 2 (arbitrary unit). The S-lens RF was set at 90 (arbitrary unit). The orbitrap resolution was 140 000. The

Automatic Gain Control (AGC) target was 3e6 and the maximum injection time was set at 250 ms. All Ion Fragmentation (AIF) experiments were done between *m/z* 100-1500 for the PSA peptide and between *m/z* 400-1500 for the 3 protein mixture over a scan range of *m/z* 100 to *m/z* 1500 for both samples, with laser (LID) and without laser (no fragmentation). The HCD parameters (collision energy CE and activation time) have been optimized in order to avoid CID fragmentation (see Results section) and were set according to the experiments. The laser power was adjusted to 500 mW. Peptide identification was performed with a top10 analysis. After a precursor scan, intact peptides were measured in the orbitrap by scanning from *m/z* 400 to *m/z* 1500 (with a resolution of 35000), the 10 most intense multiply-charged precursors (2+ to 5+) were selected for CID analysis in the C-trap (with an isolation window of 2.0 *m/z*). The normalized collision energy was set to 28. Automatic gain control (AGC) targets were 3e6 ions for the full scans (max injection time 250 ms) and 2e5 for MS/MS scans (max injection time 120 ms). Dynamic exclusion for 30 sec was used to reduce repeated analysis of the same components. The activation time was set to 3 ms for CID experiments. The resolution for the MS/MS analysis was set to 17500.

Peptide and Protein Identification

Fragmentation data were converted to peaklists using a script based on the Raw_Extract script in Xcalibur v2.4 (Thermo Fisher Scientific, San Jose, CA)[27] and the HCD data for each sample were found using Protein Prospector version v 5.10.0[28] compared to the sequences of the 3 proteins contained in the Swissprot human database (downloaded June 27, 2013; 540546 entries), to which a randomized version of all entries had been concatenated. All searches used the following parameters: mass tolerances in MS and MS/MS modes were 20 ppm and 0.2 Daltons, respectively. Trypsin was designated as the enzyme and up to two missed cleavages were allowed. Dabcyl maleimide modification of cysteine residues was designated

as a fixed modification. The considered variable modifications were N-terminal acetylation, N-terminal glutamine conversion to pyroglutamate and methionine oxidation. The maximum expected value allowed was set at up to 0.01 (protein) and 0.05 (peptide). At these thresholds any false positive identification could be observed in the search against to the concatenated database[29] for each experiment.

Peptide quantification

All peptides of the 3 protein mixture identified in a top10 analysis (HCD experiment) have been determined and quantified in each injection by using the MS1 filtering tool in skyline. The peptides have been integrated allowing a match tolerance of 0.055 *m/z* and a minimum isotope dot product (idotp=isotope distribution and its correlation between an expected and observed pattern with optimal matching resulting in an idotp value of "1") of 0.9 for at least the most intense ion of each peptide in the "no laser" injection. All integrations have been verified manually and the total area of each peptide has been reported for all precursor charge states.

Results and discussion

The aim of this work was to develop a methodology of visible photodissociation in a high resolution mass spectrometer for the specific detection of cysteine-containing peptides. The choice to irradiate in the visible range was governed by the non-absorbing property of the vast majority of natural molecules in this range, which is the case for peptides and proteins. Specific photodissociation is then expected after derivatization of the cysteine thiol group of proteins with an adequate chromophore group such as Dabcyl C2-maleimide, which exhibits a high photodissociation yield between 465 and 540 nm. We previously illustrated the

substantial reduction of interfering signals when targeting cysteine-containing peptides derivatizated with this chromophore by photo-SRM in whole plasma hydrolysate.[24] Such a specific dissociation mode should also considerably simplify data processing in the context of bottom-up proteomic experiments.

Optimization of the HCD cell parameters

In the experimental set-up, a continuous 473 nm laser beam was focused in the HCD cell of the Q-Exactive with the aim of specifically dissociating Dabcyl-grafted peptides (Figure 1). Therefore, we first sought the optimal parameters in the HCD cell which would produce a photofragmentation spectrum nearly free of collision-induced dissociation (CID) events. In the classical mode, the ions are accelerated by the HCD cell DC offset between the C-trap and HCD cell, and are fragmented by collisions with N_2. HCD employs higher energy dissociations than those used in ion trap CID enabling a wider range of fragmentation pathways.[30] The influence of the CE setting on the fragmentation pattern of the dabcyl-grafted IVGGWECEK peptide derived from PSA protein has thus been evaluated on-line in AIF mode over an *m/z* 100-1500 range. Figure 2 shows the area of the extracted chromatographic peaks reconstructed on doubly- and triply-protonated ions at *m/z* 471.318 and *m/z* 706.323, and on fragment ions at *m/z* 252.112 and *m/z* 213.159 as a function of CE value between 1 and 8 eV. First of all, we can note that a CE value above 1 eV is required to inject ions within the HCD cell as no signal is detected for CE = 1 eV. Between 2 and 3 eV CE, we observe mainly the triply- and doubly-protonated molecular ions at *m/z* 471.318 and *m/z* 706.323 (filled and open triangles, respectively). From 3 eV (CE value), fragment ions become detectable. They stem from dissociation of the peptide chain leading to an intense b_2 ion at *m/z* 213.159 (filled circle) and internal dissociation of the chromophore group yielding the ion at *m/z* 252.112 (open circle in Figure 2). Hence, a CE parameter tuned at 2 eV was thus

considered a good compromise between efficient ion transfer within the HCD cell and minimized CID events in order to finally operate in a pure photodissociation condition. As an illustration, Figure 3 depicts the AIF-MS/MS spectrum recorded between *m/z* 150 to *m/z* 1500 without laser irradiation (Figure 3a) and with laser irradiation (Figure 3b) for a CE of 2eV. As expected, only $[M+3H]^{3+}$ and $[M+2H]^{2+}$ molecular ions at *m/z* 471.318 and *m/z* 706.323 are detected when the laser is off. When the laser is turned on (Figure 3b), intense product ions arise from dissociation of the chromophore (see structure in Figure 2) yielding a specific reporter ion at *m/z* 252.112 and its complementary charge-reduced fragment ion retaining the peptide moiety $[M+H-252]^{+}$ at *m/z* 1160.434 (Figure 3b). Fragmentation of the peptide backbone is also observed mainly leading to singly-charged y_n and y_n-252 fragment ions as well as an intense b_2 and a_2 ions. y_n fragments that retain the intact chromophore are observed for n= 1 and 3 to 7, while y_n-252 fragment ions are observed for n= 5 to 7. Doubly charged $(y_8)^{2+}$, $(y_7)^{2+}$ and $(y_8\text{-}252)^{2+}$ fragment ions are also observed. Altogether, these species provide peptide sequence information. Thus, tuning the CE value to 2 eV provides a photofragmentation spectrum virtually free of CID contamination.

Since the detection of cysteine-containing peptides lies in a specific fragmentation governed by light absorption, we next measured the fragmentation yield of the derivatized IVGGWECEK peptide as a function of irradiation time from 0 ms to 200 ms (Figure 4). Using the AIF mode and because the doubly- and triply-charged molecular ions are fragmented, the photofragmentation yield, τ, has been calculated as:

$$\tau = \frac{\text{Intensity(fragments)}}{\text{Intensity(parents + fragments)}}$$

where intensity(parents) is the intensity of both $[M+3H]^{3+}$ and $[M+2H]^{2+}$ precursor ions and intensity(fragments) is the intensity of all the detected fragment ions. From 0 to 100 ms of activation time, the photofragmentation yield increases. The data can be fitted with an $A \times (1 - exp^{\frac{-x}{t}})$ equation. The photofragmentation is very efficient and after 25 ms there is a

saturation of the photofragmentation yield, which tends towards 1. The overlap between the ions and the laser beam is optimal because all the precursor ions are fragmented. An optimal 100 ms HCD cell activation time, for which almost complete photofragmentation of the derivatized peptide is observed, was retained for further experiments on mixed peptide hydrolysates analyzed in AIF mode. Note that the fragmentation yield of about 80% for a 30 ms irradiation time would probably still be sufficient to consider transposing the method to data-independent acquisition using segmented mass windows to cover a mass range.[31]

Specific detection of cysteine-containing peptides in whole trypsin hydrolysate

After defining the optimal HCD cell value at 2eV and irradiation time at 100 ms, the experimental set-up has been evaluated for the detection specificity of cysteine-containing peptides in a simple mixture of 3 proteins. Human albumin, human serotransferin and chicken lysozyme have been mixed, reduced by TCEP prior to derivatization with Dabcyl chromophore, and then digested with trypsin. Finally, 5 µL of the whole trypsin hydrolysate, which roughly correspond to 7.5 nmoles of each protein, were injected on a conventional flow reverse-phase column (i.e. 2 mm internal diameter). Figure 5a shows the superimposed total ion chromatograms (TICs) successively recorded in AIF mode between 400 and 1500 Th without (blue line) and with (black line) laser irradiation. The same retention times are obtained for the two injections. The total ion current remains constant between the two experiments, which means that the loss of signal of the photofragmented ions is offset by the increased signal of the fragment ions. On the other hand, the extracted chromatograms of the chromophore reporter ion *m/z* 252.112 (Figure 5b) clearly indicate that this diagnostic ion is only detected when the laser is turned on (blue line). Comparison with the total ion chromatograms in Figure 5a shows that this *m/z* 252.112 ion is not observed for all peptides but only for specific derivatized cysteine-containing peptides. Considering that pinpointing

cysteine-containing peptides in complex proteome could be rationalized by comparing AIF experiments with and without laser irradiation, we finally quantified the dissociation yield of 96 peptides in the hydrolysate, amongst which 39 peptides contain a cysteine tagged with the dabcyl chromophore, identified by Protein Prospector in a top 10 CID experiment (Table S1 in Supplementary Information). The dabcyl maleimide label (+391.16), implemented in the modification options of the search engine Protein Prospector, was selected as a constant modification on cysteines as we considered that the non-labeled peptides would not fragment by LID. The peptide assignment was based on the detection of fragments y and b containing or not the chromophore. The peak areas and dissociation ratio of the different charge states for all the peptides measured with and without laser irradiation are reported in Table S2 (Supplementary Information). Figure 6 shows the sum of the peak areas of the different charge states for all peptides without cysteine (a) and cysteine-containing peptides (b), with laser *versus* no laser irradiation. The peak areas of non-tagged peptides without cysteine (a) are similar when they are analyzed with and without laser irradiation since the coefficient of correlation between the two experiments shows an R^2 of 0.9918. Peptides without cysteine are clearly not affected by laser irradiation. These non-tagged precursor ions remain intact and no fragment ions are generated in AIF mode with the laser because these ions do not absorb (as shown in Figure S1 in Supplementary Information for the doubly-protonated AVMDDFAAFVEK non-cysteine peptide detected at *m/z* 671.823). On the other hand, the laser irradiation efficiently induces photodissociation of tagged cysteine-containing peptides (Figure 6b), leading to, on average, an 80% decrease of the protonated peptide signal (Table S2).

Perspective for proteomic applications.

The question rises now about how this specific photodissociation of cysteine-containing peptides may be exploited in the context of proteomics based on a bottom-up strategy. Generally speaking, there is no interest to use photodissociation for performing proteomic discovery in conventional data dependent acquisition mode (DDA). Indeed, in DDA only the major peaks are fragmented and would not necessarily correspond to derivatized cysteine-containing peptides, leading to non-informative spectra. Moreover, the relative long irradiation time to achieve high fragmentation yield would result in under sampling of precursor ions. On the other hand, the high fragmentation specificity provided by visible photodissociation mode is especially attractive for data independent acquisition mode (DIA) for which any possibility of reducing and rationalizing the fragmentation ion pattern should facilitate data interpretation and peptide/protein assignment. Figure 7 illustrates how raw data might be processed to extract informative specific signals. Herein are presented the AIF spectra recorded at retention times 12.8 and 21.5 min without laser (Figure 7a and 7d) and with laser irradiation for 100 ms (Figure 7b and 7e), and the resulting spectra after subtraction of both (Figure 7c and 7f). These latter exhibit species with intense negative intensity at *m/z* 461.915 (Figure 7c) and *m/z* 553.937 (Figure 7f) corresponding to triply protonated molecular ions of the two derivatized cysteine-containing peptides C*ELAAAMKR and GYSLGNWVC*AAK that have been specifically fragmented by LID. In contrast, the intensities of ions detected at *m/z* 756.121, 1133.648, 756.149 and 1133.618 in the AIF spectra recorded with and without laser are markedly reduced after subtraction, signifying that there are not affected by the laser and do not contain derivatized cysteine residue. Similar features are retrieved in the subtracted spectra provided as supplementary information for cysteine-containing peptides (Figure S2) and peptides free of cysteine residue (Figure S3). Thus, subtracted spectra will allow pinpointing only accurate masses of cysteine-containing peptides specifically fragmented in LID. Furthermore, the AIF subtracted spectra at retention

times where cysteine-containing peptides are eluted contain informative fragment ions, i.e. reporter ion at *m/z* 252.112 and backbone peptide cleavages leading to y, b and y-252 type ions. In the future, effective implementation of visible photodissociation in DIA mode would first consist in synthesizing a cysteine-containing peptide library, attributing a relative retention time for each of them[32] and recording visible photodissociation spectral bank. Then, comparison of experimental chromatograms and spectra with this database will allow a straightforward peptide assignment.

Conclusions

By implementing laser irradiation at 473 nm in a Q-Exactive Orbitrap instrument, we were able to show discriminating detection of cysteine-containing peptides grafted with a Dabcyl group following laser irradiation in the visible range. Tuning the CE value of the HCD cell at 2eV during laser irradiation provides fragmentation spectra free of CID events. In All Ion Fragmentation mode, a 100 ms irradiation time was shown to be sufficient for a high dissociation yield while remaining compatible with a liquid chromatography time scale separation for correct peak definition. Using these optimized parameters, detection of cysteine-containing peptides in trypsin hydrolysate of a three-protein mixture was rationalized from the comparison of the reconstructed ion chromatograms of the intense reporter ion at *m/z* 252.112 recorded with and without laser irradiation. The interest of this unique experimental set-up is currently under evaluation towards large-scale specific detection of the subset of cysteine-containing peptides by DIA mode in whole cellular proteome hydrolysate in the context of oxidative stress studies. Finally, implementing a specific photodissociation step in DIA mode would allow a straightforward peptide and protein assignment and quantification using a specific database search restricted to derivatized cysteine-containing peptides.

Acknowledgment

The authors would like to thank Andreas Kuehn and Rose Bjoern from Thermo Fisher Scientific for providing the new tune software version allowing us to edit the HDC parameters, and the French Agence National de la Recherche for the funding of this photo-SRM project (ANR-11-BSV5-003-01). The research leading to these results has received funding from the European Research Council under the European Union's Seventh Framework Programme (FP7/2007-2013 Grant agreement N°320659).

References

1. M. H. Elliott, D. S. Smith, C. E. Parker and C. Borchers, *J. Mass Spectrom.*, 2009, **44**, 1637-1660.
2. L. Anderson and C. L. Hunter, *Mol. Cell. Proteomics*, 2006, **5**, 573-588.
3. R. A. Zubarev, K. F. Haselmann, B. Budnik, F. Kjeldsen and F. Jensen, *Eur. J. Mass Spectrom.*, 2002, **8**, 337-349.
4. J. Langridge, J. Brown, S. Mohammed, N. Taouatas, I. D. G. Campuzano and A. J. R. Heck, *Mol. Cell. Proteomics*, 2009, S25-S25.
5. N. Taouatas, A. F. M. Altelaar, M. M. Drugan, A. O. Helbig, S. Mohammed and A. J. R. Heck, *Mol. Cell. Proteomics*, 2009, **8**, 190-200.
6. Y. Tian, Y. Zhou, S. Elliott, R. Aebersold and H. Zhang, *Nat. Protoc.*, 2007, **2**, 334-339.
7. Y. Zhou, R. Aebersold and H. Zhang, *Anal. Chem.*, 2007, **79**, 5826-5837.
8. S. P. Gygi, B. Rist, S. A. Gerber, F. Turecek, M. H. Gelb and R. Aebersold, *Nat. Biotechnol.*, 1999, **17**, 994-999.
9. V. Larraillet, R. Antoine, P. Dugourd and J. Lemoine, *Anal. Chem.*, 2009, **81**, 8410-8416.
10. J. A. Madsen, D. R. Boutz and J. S. Brodbelt, *J. Proteome Res.*, 2010, **9**, 4205-4214.
11. J. P. Reilly, *Mass Spectrom. Rev.*, 2009, **28**, 425-447.
12. M. C. Crowe and J. S. Brodbelt, *Anal. Chem.*, 2005, **77**, 5726-5734.
13. R. Antoine and P. Dugourd, *J. Chem. Phys.*, 2011, **13**, 16494-16509.
14. L. Joly, R. Antoine, M. Broyer, P. Dugourd and J. Lemoine, *J. Mass Spectrom.*, 2007, **42**, 818-824.
15. A. Agarwal, J. K. Diedrich and R. R. Julian, *Anal. Chem.*, 2011, **83**, 6455-6458.
16. J. K. Diedrich and R. R. Julian, *Anal. Chem.*, 2010, **82**, 4006-4014.
17. J. K. Diedrich and R. R. Julian, *Anal. Chem.*, 2011, **83**, 6818-6826.
18. J. R. Cannon, M. B. Carnmarata, S. A. Robotham, V. C. Cotham, J. B. Shaw, R. T. Fellers, B. P. Early, P. M. Thomas, N. L. Kelleher and J. S. Brodbelt, *Anal. Chem.*, 2014, **86**, 2185-2192.
19. J. B. Shaw, W. Li, D. D. Holden, Y. Zhang, J. Griep-Raming, R. T. Fellers, B. P. Early, P. M. Thomas, N. L. Kelleher and J. S. Brodbelt, *J. Am. Chem. Soc.*, 2013, **135**, 12646-12651.
20. J. A. Madsen, H. Xu, M. R. Robinson, A. P. Horton, J. B. Shaw, D. K. Giles, T. S. Kaoud, K. N. Dalby, M. S. Trent and J. S. Brodbelt, *Mol. Cell. Proteom.*, 2013, **12**, 2604-2614.
21. V. C. Cotham, Y. Wine and J. S. Brodbelt, *Anal. Chem.*, 2013, **85**, 5577-5585.
22. J. P. O'Brien, J. M. Pruet and J. S. Brodbelt, *Anal. Chem.*, 2013, **85**, 7391-7397.
23. J. R. Aponte, L. Vasicek, J. Swaminathan, H. Xu, M. C. Koag, S. Lee and J. S. Brodbelt, *Anal. Chem.*, 2014, **86**, 6237-6244.
24. Q. Enjalbert, M. Girod, R. Simon, J. Jeudy, F. Chirot, A. Salvador, R. Antoine, P. Dugourd and J. Lemoine, *Anal. Bioanal. Chem.*, 2013, **405**, 2321-2331.
25. P. Giron, L. Dayon and J.-C. Sanchez, *Mass Spectrom. Rev.*, 2011, **30**, 366-395.
26. S. H. Wang, X. Zhang and F. E. Regnier, *J. Chromatogr. A*, 2002, **949**, 153-162.
27. S. Guan, J. C. Price, S. B. Prusiner, S. Ghaemmaghami and A. L. Burlingame, *Mol Cell Proteomics*, 2011, **10**, M111 010728.
28. R. J. Chalkley, P. R. Baker, K. F. Medzihradszky, A. J. Lynn and A. L. Burlingame, *Mol Cell Proteomics*, 2008, **7**, 2386-2398.
29. J. E. Elias and S. P. Gygi, *Nat Methods*, 2007, **4**, 207-214.
30. M. P. Jedrychowski, E. L. Huttlin, W. Haas, M. E. Sowa, R. Rad and S. P. Gygi, *Mol. Cell. Proteomics*, 2011, **10**.

31. B. C. Collins, L. C. Gillet, G. Rosenberger, H. L. Roest, A. Vichalkovski, M. Gstaiger and R. Aebersold, *Nat. Methods*, 2013, **10**, 1246-+.
32. C. Escher, L. Reiter, B. MacLean, R. Ossola, F. Herzog, J. Chilton, M. J. MacCoss and O. Rinner, *Proteomics*, 2012, **12**, 1111-1121.

Figure 1. Schematic of the experimental set-up of photodissociation in the Q-Exactive mass spectrometer.

Figure 2. Area of the extracted chromatographic peaks of *m/z* 471 ($[M+3H]^{3+}$) (▲), *m/z* 706 ($[M+2H]^{2+}$) (Δ), *m/z* 252 (○) and *m/z* 213 (●) fragment ions according to the collision energy (CE) without laser irradiation.

Figure 3. AIF-MS/MS spectra from *m/z* 150 to *m/z* 1500 of Dabcyl C2 maleimide grafted onto the cysteine-containing IVGGWECEK peptide a) without laser and b) with laser at 473 nm, using CE 2 eV and irradiation time of 100 ms.

Figure 4. Photofragmentation yield at 473 nm of Dabcyl C2 maleimide grafted onto the cysteine-containing IVGGWECEK peptide 2+ and 3+ ions as a function of the activation time in the HCD cell (collision energy 2 eV).

Figure 5. a) Total ion chromatogram of the AIF-MS/MS of a 3 protein sample during 50 min with a gradient of acetonitrile 20-45% and b) Extracted chromatogram of the reporter ion *m/z* 252, with (blue) or without (black) laser.

Figure 6. Areas of all non-cysteine peptides a) and cysteine peptides b) with laser vs. without laser.

Figure 7. AIF spectra at RT= 12.8 min a) without laser and b) with laser. c) Subtract laser-no laser AIF spectrum at RT= 12.8 min. AIF spectra at RT= 21.5 min d) without laser and d) with laser. f) Subtract laser-no laser AIF spectrum at RT= 21.5 min.

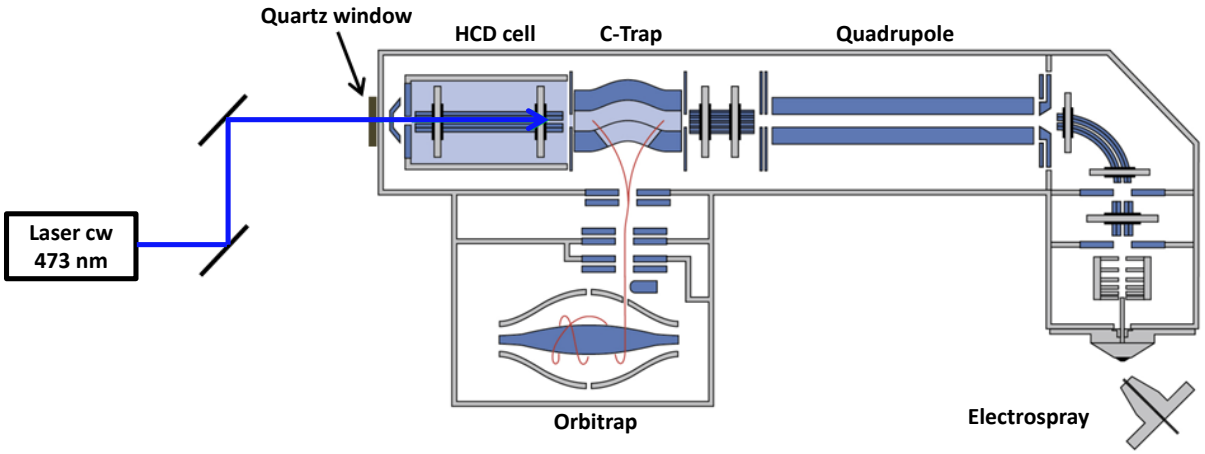

Figure 1.

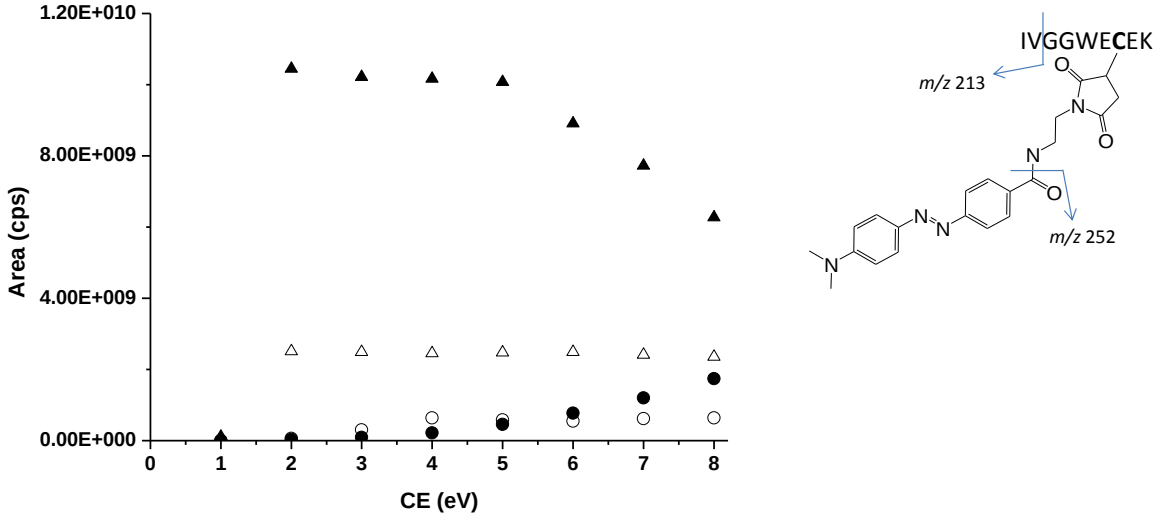

Figure 2.

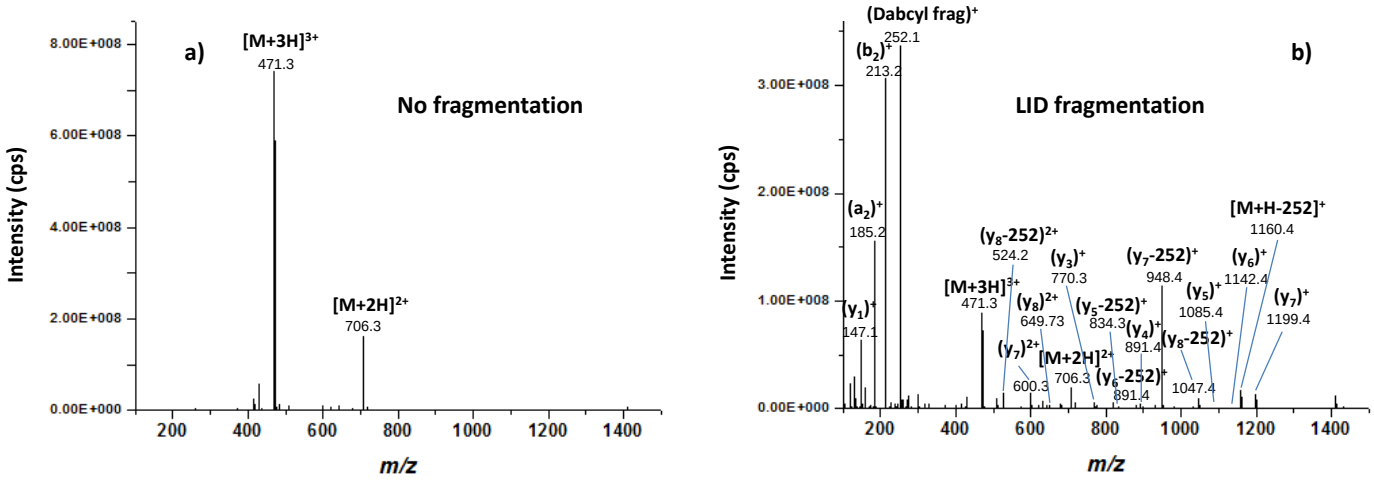

Figure 3.

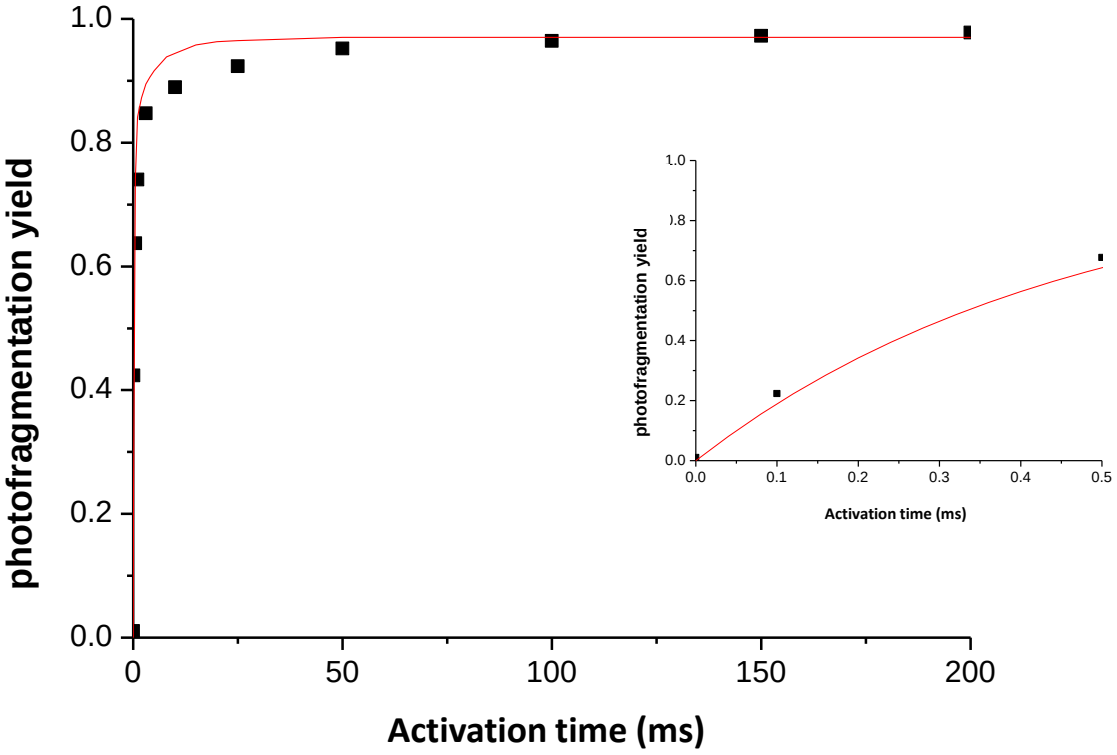

Figure 4.

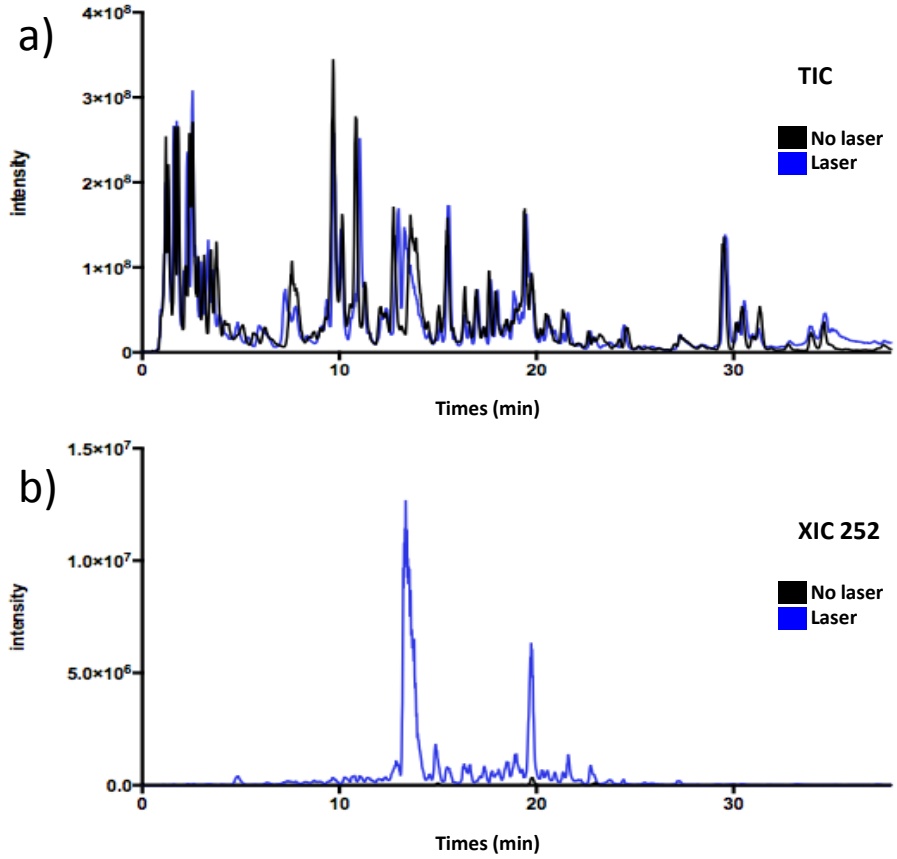
a)
4×10^8
3×10^8
2×10^8
1×10^8
0
intensity
TIC
No laser
Laser
0
10
20
30
Times (min)
b)
1.5×10^7
1.0×10^7
5.0×10^6
0.0
intensity
XIC 252
No laser
Laser
0
10
20
30
Times (min)

Figure 5

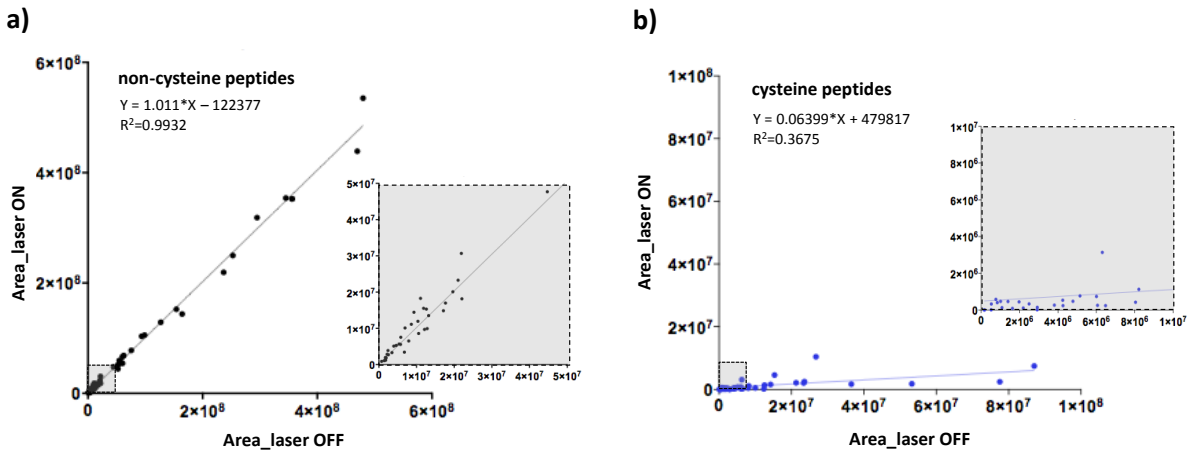
a)
non-cysteine peptides
Y = 1.011*X – 122377
R²=0.9932
Area_laser ON
Area_laser OFF
b)
cysteine peptides
Y = 0.06399*X + 479817
R²=0.3675
Area_laser ON
Area_laser OFF

Figure 6

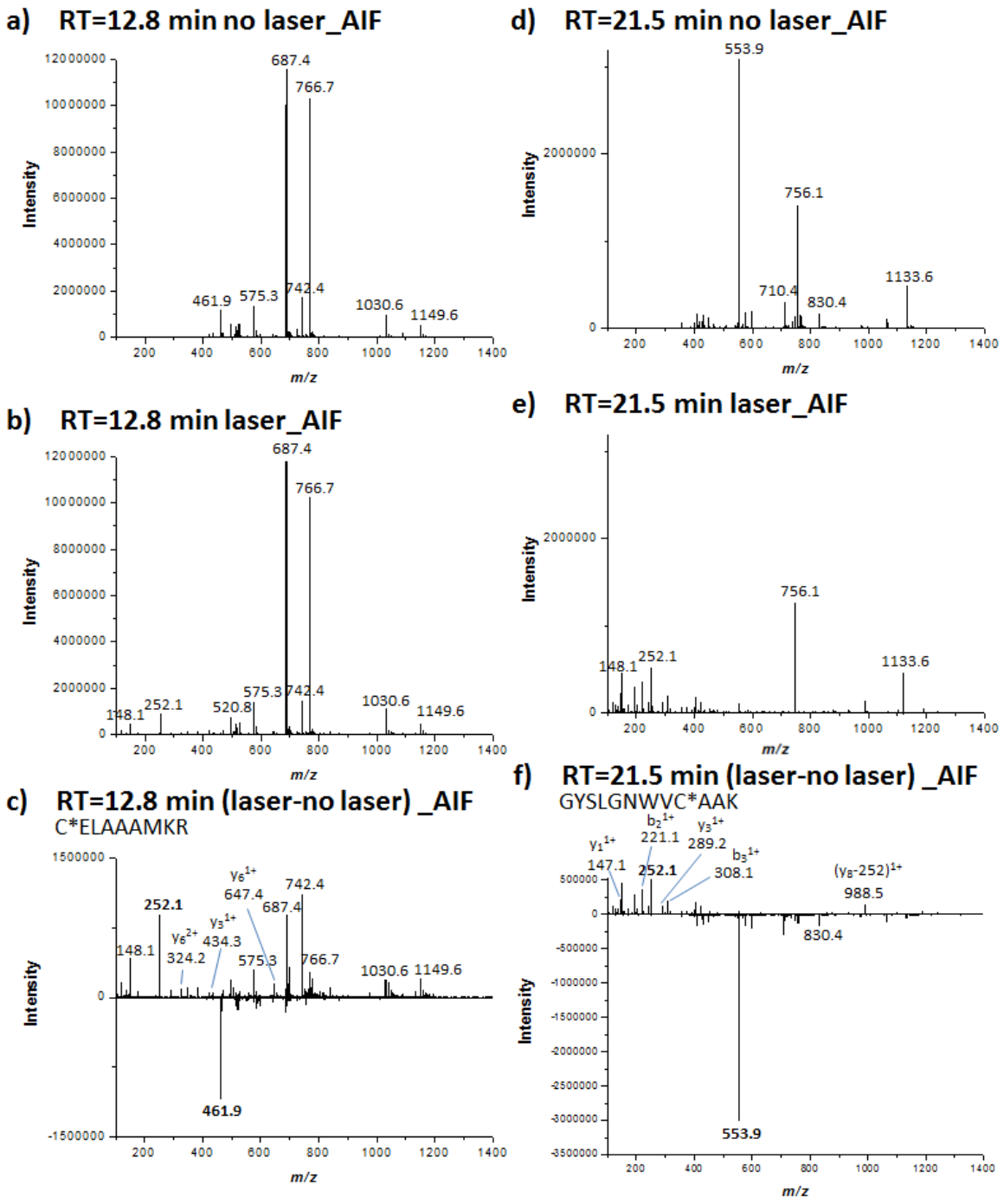
a) RT=12.8 min no laser_AIF
687.4
766.7
461.9
575.3
742.4
1030.6
1149.6
Intensity
m/z
b) RT=12.8 min laser_AIF
687.4
766.7
148.1
252.1
520.8
575.3
742.4
1030.6
1149.6
Intensity
m/z
c) RT=12.8 min (laser-no laser) _AIF
C*ELAAAMKR
252.1
148.1
324.2
434.3
647.4
687.4
742.4
575.3
766.7
1030.6
1149.6
461.9
Intensity
m/z
d) RT=21.5 min no laser_AIF
553.9
756.1
710.4
830.4
1133.6
Intensity
m/z
e) RT=21.5 min laser_AIF
756.1
148.1
252.1
1133.6
Intensity
m/z
f) RT=21.5 min (laser-no laser) _AIF
GYSLGNWVC*AAK
147.1
221.1
252.1
289.2
308.1
988.5
830.4
553.9
Intensity
m/z

Figure 7